

Self Assemble Structure of Amphiphilic Di-block Copolymer Having Azobenzene Moieties

Hirohisa Yoshida[#], Kazuhiro Watanabe^{*}, Ryoko Watanabe^{*}, Tomokazu Iyoda^{*,#}

Department of Applied Chemistry, Graduate School of Engineering, Tokyo Metropolitan University, Hachioji, Tokyo 192-0397 JAPAN

Fax: 81-426-77-2821, e-mail: yoshida-hirohisa@c.metro-u.ac.jp

^{*} Chemical Research Laboratory, Tokyo Institute of Technology, Nagatsuda, Yokohama 226-8503, JAPAN,

Fax: 81-45-924-5247, e-mail: iyoda@res.titech.ac.jp

[#] CREST (JST), JAPAN

The phase transitions and the nanoscale ordered structure of amphiphilic di-block copolymer consisted with poly(ethylene oxide) (PEO) and azobenzene derivative methacrylate (AZO) were investigated by TEM and the simultaneous DSC-XRD utilized the synchrotron radiation. TEM observation suggested that PEO-AZO di-block copolymer formed the highly ordered hexagonal-packed PEO cylinder structure in nanoscale due to the micro phase separation. Four phase transitions were assigned to the melting of PEO, the melting, the smectic transition and the isotropic transition of AZO moieties from the observation of DSC-XRD. The order of micro phase separation structure was influenced by annealing at the smectic phase and the isotropic phase. The SAXS observation indicated that the high ordered hexagonal-packed cylinder structure formed continuously from the surface to the bulk region. The characteristic hexagonal-packed cylinder structure was observed in wide AZO composition and temperature range as the equilibrium structure. PEO-AZO formed the hexagonal-packed cylinder structure to compensate the conformational entropy loss by reducing the area of interface between PEO and AZO domains.

Key words: Di-block copolymer, Micro phase separation, Hexagonal phase, Liquid crystal, Smectic phase

1. Introduction

Block copolymers can self-assemble into nanoscale ordered structures due to microphase separation. For di-block copolymers with fine controlled block sequences, lamellar, hexagonal-packed cylinder, bicontinuous cubic gyroid and body-centered cubic structures are confirmed as equilibrium structures. These nanoscale ordered structures are formed mainly by the results of repulsive interaction between copolymer components. The ordered structures caused by micro phase separation are reported not only A-B di-block but also A-B-A tri-block copolymers and these blends with homopolymers [1-4]. These previous works are reported for the copolymers with couples of component having weak repulsive interaction such as styrene and isoprene. The nanoscale ordered structure is formed as a result of micro phase separation at the isotropic liquid state for these block copolymers.

We have reported the nanoscale ordered structure and phase transitions of amphiphilic di-block copolymer consisted with hydrophilic and hydrophobic sequences having azobenzene moieties [5-7]. The di-block copolymers composed of block sequences including azobenzene moieties, which acts as a mesogen of side chain type liquid crystalline polymer, form the hexagonal-packed cylinder phase as a nanoscale ordered structure, and demonstrate

several phase transitions including liquid crystalline and isotropic transitions [5, 6]. The di-block copolymers containing a liquid crystalline state in the micro-phase separation phase tended to form hexagonal-packed cylinder rather than to form body-centered cubic as a nanoscale ordered structure [8, 9].

In this study, the phase transition behavior of amphiphilic di-block copolymer was investigated by the simultaneous DSC-XRD method utilizing the synchrotron X-ray radiation beam in order to investigate the relationship between the nanoscale ordered structure and the phase equilibrium of separated phases.

2. Experimental

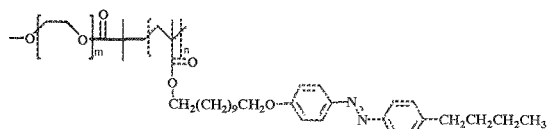
Amphiphilic di-block copolymers consisted with poly(ethylene oxide) (PEO) and azobenzene derivative methacrylate, 11-[4-(4-butylphenyl-azo)phenoxy]-undecyl methacrylate, (AZO) were prepared by the atom transfer radical polymerization [7]. Block sequences of PEO and AZO were determined by ¹H-NMR and were shown as P_nA_m (Scheme1) with degrees of polymerization of each component (n and m). The degrees of polymerization of PEO sequence used in this experiment were 40, 114 and 454. The weight fraction of AZO (f_{AZO}) of di-block copolymer used in this study was from 0.6 - 0.9.

The transmission electron microscopic observation (TEM) was carried out by JEOL EX

200 operating at 200 kV. The sample for TEM was prepared by the solvent casting method on amorphous carbon and was stained by vapor of 1 wt% aqueous solution of ruthenium oxide

The DSC observation was done by Seiko Instruments DSC model 6200 equipped with the cooling apparatus at scanning rate from 10 – 1 Kmin⁻¹ under dry nitrogen gas flow.

The simultaneous DSC-XRD measurements were carried out at the beam line 10C, Photon Factory, High Energy Accelerator Research Organization, Tsukuba, Japan. The wavelength of monochromatic X-ray for DSC-XRD was 0.1488 nm. The scattering X-ray was detected by a one-dimensional position sensitive proportional counter (PSPC, 512 channels, Rigaku Co. Ltd.). The distance between sample and PSPC was 550 mm, which covered $1.02 \text{ nm} < s^{-1} = (2\pi/q)^{-1} = (2\sin\theta/\lambda)^{-1} < 60.8 \text{ nm}$. The simultaneous DSC-XRD measurement was carried out by setting the simultaneous DSC [10] on the small X-ray scattering optics. The heating rate of DSC was 2 Kmin⁻¹, and XRD profiles were stored for each 1 K. The temperature and enthalpy were calibrated by pure indium and tin. The sample sandwiched with two thin aluminum foils and cramped in an aluminum sample vessel [11]. Sample weight used was about 5 mg.



Scheme 1

3. Results and discussions

3.1 Nanoscale order structure

The transmission electron microscopic (TEM) image of nanoscale order structure of P114A45 is shown in Fig.1 (A). The sample was annealed at 140 °C for 24 hrs. Black spots aligned hexagonally are the stained PEO domains existing in the unstained AZO matrix. The diameter of PEO cylinder was about 7 nm, which decreased slightly with increasing AZO weight fraction (f_{AZO}). The distance between PEO cylinders was about 10 nm, which increased with the increase of f_{AZO} . The hexagonal-packed cylinder structure was observed in the f_{AZO} range from 0.6 to 0.9, which was considerably wider range comparing with the phase diagram for di-block copolymers having weak repulsive interactions. Fourier transformation profile of TEM image in the area of $1 \mu\text{m}^2$ suggested the monodomain consisting with the highly ordered hexagonal-packed cylinder as shown in Fig.1 (B). The ultra-thin cross sectional TEM view of P114A45 indicated that PEO cylinders passed through about $2 \mu\text{m}$ thickness film. These facts suggested that long PEO cylinders with about 7 nm diameter and $2 \mu\text{m}$ length were packed in the nanoscale hexagonal unit cell.

The highly ordered hexagonal-packed cylinder

structure was also supported by the SAXS observation of higher order diffraction peaks at the position of $1, \sqrt{3}, \sqrt{4}, \sqrt{7}$ and $\sqrt{9}$. The size of hexagonal unit cell evaluated by SAXS was same to the value estimated by TEM observation. The nanoscale ordered structure was influenced by both copolymer content and annealing temperature. With increasing the annealing temperature, the fine nanoscale ordered structure was formed.

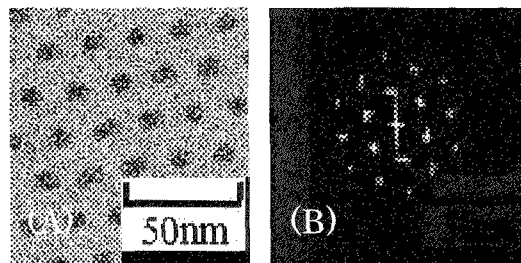


Fig.1 TEM image (A) and 2-dimensional FT imaging (B) for P114A45

3.2 Phase transitions

DSC heating curves of block copolymers with various block contents are shown in Fig.2. Four phase transitions observed during heating were assigned to the melting of PEO, two kinds of transitions relating to the liquid crystalline states (A and B in Fig.2) and the isotropic phase transition from low temperature side. PEO homopolymer showed about 10 °C super-cooling of crystallization on cooling, however, the degree of super-cooling for PEO domain of block copolymer was more than 30 °C. This fact suggested that the phase transition of PEO existed in the phase separated domain was influenced by the copolymer sequence of AZO. The melting entropy of PEO was about $10 - 15 \text{ JK}^{-1} \text{ mol}^{-1}$, the crystallinity of PEO in PnAm di-block copolymer was about 30 – 60 % using the thermodynamic melting entropy for PEO [12].

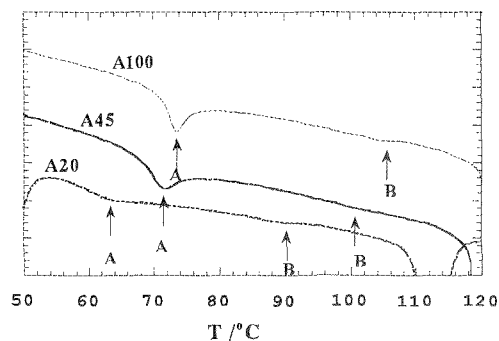


Fig.2 DSC heating curves of P114A20, P114A45 and P114A100 at 5 Kmin⁻¹.

The isotropic transition temperature of azobenzene moieties was influenced slightly by PEO block component in the f_{AZO} range from 0.7 to 0.9, however, the melting entropy increased with the increase of f_{AZO} at the same f_{AZO} range. The isotropic transition entropies evaluated on heating and cooling were almost the same, and were about $3 - 8 \text{ JK}^{-1} \text{ mol}^{-1}$ in the f_{AZO} range from 0.7 to 0.9. These entropy values are similar to that of transition from smectic A to isotropic liquid for low molecular weight liquid crystalline materials, such as 4-n alkoxy-3 nitrophenyl 4-carboxylic acids [13, 14].

Two phase transitions shown as A and B in Fig.2 were also influenced by f_{AZO} , however showed a small degree of super cooling within 1°C . The phase transition A was assigned to the melting of azobenzene moiety. The transition entropy of the transition A indicated that more than 90 % of azobenzene moieties were in the super-cooled state of liquid crystalline state in this experiment. Thus the AZO matrix of the nanoscale ordered structure was in the thermodynamic equilibrium state and in the flexible state. The transition B was the broad endothermic transition, which started immediately after the transition A and the transition temperature range was over 20°C .

3.3 Temperature change of nanoscale ordered structure.

The stacked XRD profile change for P114A45 observed by the simultaneous DSC-XRD is shown in Fig.3. Two diffraction peaks observed at low scattering vector (q) range below 0.9 nm^{-1} were assigned to the (100) and (110) planes of hexagonal-packed nanoscale ordered structure ($(d_{110})^{-1} = \sqrt{3}(d_{100})^{-1}$). The diffraction peak intensities of the (100) and (110) planes were strong when the PEO was crystallized because of the large electron density difference between the PEO cylinder domain and the AZO matrix. The peak intensities of diffractions from the hexagonal nanoscale ordered structure decreased after the melting of PEO, however, the hexagonal structure remained. In the temperature range above the isotropic transition, these two diffraction peaks were observed clearly again.

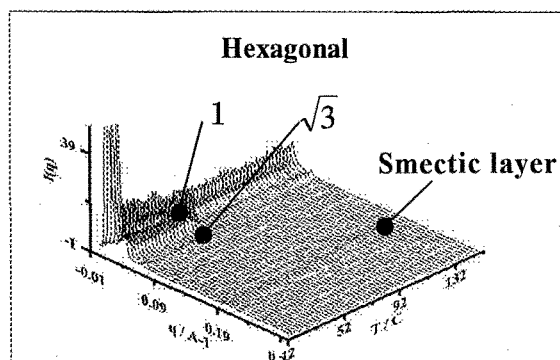


Fig.3 XRD profile change for P114A45 obtained by DSC-XRD on heating at 5 Kmin^{-1} .

The diffraction peaks of nanoscale ordered structure observed by the static XRD measurement suggested that the high ordered hexagonal-packed long cylinder structure was the equilibrium structure of P114A45 at the temperature range from 0 to 140°C . TEM and XRD results indicated that the long PEO cylinder islands existed at hexagonal lattice in the smectic liquid crystalline AZO matrix as shown in Fig.1 (A) was the fine structure of P114A45.

3.4 Temperature change of liquid crystalline structure.

The broad diffraction peak at 2 nm^{-1} ($d = 3.1 \text{ nm}$) in Fig.3 was due to the smectic layer of liquid crystalline phase, because this diffraction peak disappeared at the isotropic transition. The smectic layer distance was evaluated by the Gauss distribution fitting of diffraction peak.

The smectic layer distance evaluated from XRD profiles obtained by DSC-XRD was plotted with DSC curve for P114A20 in Fig.4. The distance and the diffraction intensity of smectic layer were changed at the transitions A and B. The smectic layer distance at temperature between the transition B and the isotropic transition scarcely changed even at the liquid crystalline state, and 3.3 nm was corresponded to the length of extended azobenzene moieties. The liquid crystalline state between the transition B and the isotropic transition was a smectic A phase in which the mesogenic azobenzene moieties aligned perpendicular to the smectic layer.

The thermal expansion coefficient evaluated from the smectic layer distance change at temperature between transitions A and B was $1.6 \times 10^{-3} \text{ K}^{-1}$. This value was almost ten times larger than the thermal expansion coefficient of the rubbery state of polymer. This large value was due to change the tilt angle of mesogenic azobenzene unit, that is, the transition B was the transition from smectic C to smectic A.

The liquid crystalline phase between the transitions A and B with the constant smectic layer distance (3.15 nm) was the smectic C phase.

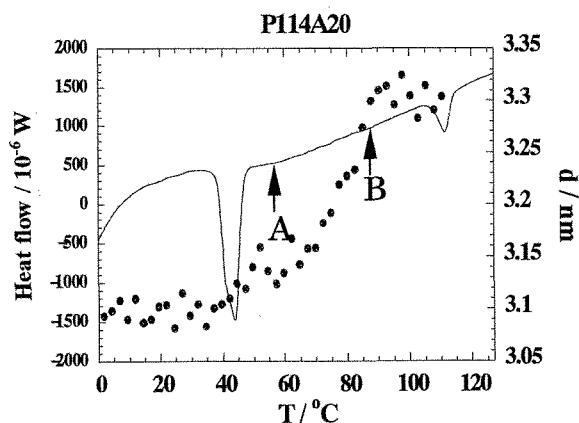


Fig.4 Temperature change of smectic layer distance and DSC curve observed by DSC-XRD on heating at 5 Kmin^{-1} .

3.5 Gibbs free energy of ordered structure formation

Gibbs free energy change per molecule (Δg) for the formation of ordered structure from the random mixing state of block sequences is described as follows.

$$\Delta g = \Delta h - T\Delta S_{\text{inf}} - T\Delta S_{\text{conf}} \quad (1)$$

Here, ΔS_{inf} and ΔS_{conf} indicate the entropy change due to the orientation of connection point between block sequences and the conformational contribution of each sequences, respectively. Δh is the enthalpy contribution of the coagulation state formation from the random mixing state, and is rewritten as follows using a thickness of interface (d_i) and an interface area per polymer chain (a_p).

$$\Delta h = -kT\chi N_{AB}\phi_A(1-\phi_A) + kT\chi \frac{a_p d_i}{v_c} \quad (2)$$

Here, k , N_{AB} , χ , ϕ_A and v_c indicate Boltzmann constant, a total number of repeating units A and B, an interaction parameter between A and B sequences, a volume fraction of A sequence and an average unit volume of component, respectively. Two entropic contributions on Gibbs free energy ΔS_{inf} and ΔS_{conf} are described as follows.

$$\Delta S_{\text{inf}} \approx k \ln \frac{d_i}{d_{AB}} \quad (3)$$

$$\Delta S_{\text{conf}} \approx -kb^2 \left(\frac{d_{AB}}{R_0} \right)^2 \quad (4)$$

Here, d_{AB} is a distance between micro domains A and B, b is a constant and R_0 is an end to end distance of block copolymer in the random mixing state.

For the equilibrium value of a_p from equations (2), (3) and (4), the following relationship is obtained [15].

$$d_{AB}^3 = \frac{N_{AB}^3 v_c^3}{a_p^3} \approx \chi d_i v_c^{2/3} N_{AB}^2 \quad (5)$$

Thus, the value of 2/3 is obtained as a power of the relationship between d_{AB} and N_{AB} from Gibbs free energy change of nanoscale ordered structure formation. The relationship between Bragg spacing of hexagonal (100) (d_{AB}) of nanoscale ordered structure evaluated at

room temperature and the degree of polymerization (N_{AB}) are shown in Fig. 5. The power obtained from the relationship between d_{AB} and N_{AB} was 0.7, which was larger than the value expected from equation (5). For di-block copolymer containing the liquid crystalline state, the conformational entropy loss in equation (1) from the liquid crystalline phase is larger than the contribution from the liquid state. In order to compensate the conformational entropy loss, the contribution of interface entropy loss decreases to decrease Gibbs free energy change. This is one of the reasons why PnAm di-block copolymer forms the hexagonal order structure rather than the body centered-cubic structure.

References

- [1] T. Hashimoto, M. Fujimura, and H. Kawai, *Macromolecules*, **13**, 1660 (1980)
- [2] S. Koizumi, H. Hasegawa, and T. Hashimoto, *Makromol. Chem. Macromol.Symp.*, **62**, 75 (1992)
- [3] D. Yamaguchi, J. Bodycomb, S. Koizumi, and T. Hashimoto, *Macromolecules*, **32**, 5884 (1999)
- [4] Y. Matsushita, J. Suzuki, N. Takabayashi, N. Torikai, M. Nomura, I. Noda, *Macromolecules*, **30**, 2378 (1998)
- [5] Y. Tian, K. Watanabe, X. Kong, J. Abe, and T. Iyoda, *Macromolecules*, **35**, 3739 (2002)
- [6] K. Watanabe, H. Yoshida, Y. Tian, S. Asaoka, and T. Iyoda, *Polym. Prep. Jpn.*, **51**, 2421 (2002)
- [7] K. Watanabe, Y. Tian, H. Yoshida, S. Asaoka, and T. Iyoda, *Trans. Materials Res. Soc. Jpn.*, **28**, 553 (2003)
- [8] H. Yoshida, K. Watanabe, R. Watanabe, Y. Tian, S. Asaoka, and T. Iyoda, *Polym. Prep. Jpn.*, **51**, 2150 (2002)
- [9] R. Watanabe, K. Watanabe, H. Yoshida, and T. Iyoda, *Polym. Prep. Jpn.*, **52**, 2577 (2002)
- [10] H. Yoshida, *Thermochimica Acta*, **267**, 239 (1995)
- [11] H. Yoshida, R. Kinoshita, Y. Teramoto, *Thermochimica Acta*, **264**, 173 (1995)
- [12] B. Wunderlich, *Polym. Eng. Sci.*, **18**, 431 (1987)
- [13] K. Saito, A. Sato, and M. Sorai, *Liquid Crys.*, **25**, 525 (1998)
- [14] K. Saito and M. Sorai, *Ekisyo.*, **5**, 20 (2001)
- [15] G. Strobl, *The Physics of Polymer*, Springer (Berlin) (1997) p.131-133.

(Received October 10, 2003; Accepted January 31, 2004)

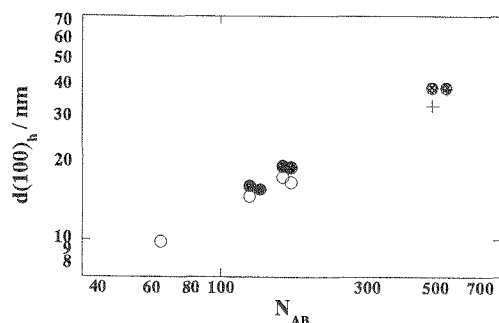


Fig.5 Relationship between Bragg spacing of hexagonal (100) and degree of polymerization of PnAm (N_{AB})